INSPYRE
Investigations Supporting MOX Fuel Licensing in ESNII Prototype Reactors

EERA JPNM
JOINT PROGRAMME ON NUCLEAR MATERIALS

D6.5 – Improved models of melting temperature and thermal conductivity for mixed oxide fuels doped with low minor actinide contents

A. Magni (ENEA, POLIMI), P. Van Uffelen, A. Schubert (JRC),
L. Luzzi (POLIMI), P. Del Prete, A. Del Nevo (ENEA)

Version 1 – 24/09/2022

The INSPYRE project has received funding from the EURATOM research and training programme 2014-2018 under Grant Agreement No 754329.

Document type	Deliverable
Document number	D6.5 version 1
Document title	Improved models of melting temperature and thermal conductivity for mixed oxide fuels doped with low minor actinide contents
Authors	A. Magni (ENEA, POLIMI), P. Van Uffelen, A. Schubert (JRC), L. Luzzi (POLIMI), P. Del Prete, A. Del Nevo (ENEA)
Release date	24/09/2022
Contributing partners	ENEA, POLIMI, JRC-Karlsruhe
Dissemination level	Public

Version	Short description	Main author	WP leader	Coordinator
1	First release	A. Magni (ENEA, POLIMI) 23/09/2022	A. Del Nevo (ENEA) 23/09/2022	M. Bertolus (CEA) 24/09/2022

SUMMARY

Recycling and burning minor actinides (MA, e.g., americium, neptunium) in mixed-oxide (MOX) nuclear fuel is a strategic option for fast reactor concepts of Generation IV to improve the sustainability of nuclear energy by reducing ultimate radioactive waste and improving the exploitation of fuel resources.

Thermal conductivity and melting temperature are fundamental properties of nuclear fuels, since they determine the fuel temperature profile and the melting safety margin, respectively and affect the overall fuel performance under irradiation. The available literature on thermal properties of Am or Np-containing MOX, both experimental data and models, is currently scarce. Moreover, state-of-the-art fuel performance codes (FPCs), e.g., GERMINAL and TRANSURANUS, do not account for the effects of minor actinides on MOX fuel properties.

This deliverable presents the development and validation of original correlations for the thermal conductivity and melting temperature of minor actinide-bearing MOX $(U,Pu,Am,Np)O_{2-x}$ based on available literature data. These correlations are derived by extending those obtained in the project for U-Pu MOX fuels with the inclusion of the effect of Am and Np content, while preserving the physically-grounded formulation depending on the most relevant parameters. Ways to improve these correlations further in the future are also discussed

CONTENT

SUMMARY 2
CONTENT 3
GLOSSARY 4
1 INTRODUCTION 5
2 LITERATURE REVIEW ON THERMAL PROPERTIES OF MA-MOX 6
2.1 Melting temperature of MA-MOX 6
2.1.1 Available data 6
2.1.2 Available correlations 7
2.2 Thermal conductivity of MA-MOX 7
2.2.1 Available data 7
2.2.2 Available correlations 8
3 MODELLING OF MELTING TEMPERATURE OF MA-MOX 9
3.1 Fitting dataset 9
3.2 Development of a correlation for MA-MOX melting temperature 11
4 MODELLING OF THERMAL CONDUCTIVITY OF MA-MOX 15
4.1 Fitting dataset 15
4.2 Development of a correlation for MA-MOX thermal conductivity 15
5 CONCLUSION AND FUTURE DEVELOPMENTS 22
REFERENCES 23

GLOSSARY

BMH	Born-Mayer-Huggins (potential)
CALPHAD	CAlculation of PHAse Diagrams
ENEA	Agenzia nazionale per le nuove tecnologie,l'energia e lo sviluppo economico sostenibile
ESNII	European Sustainable Nuclear Industrial Initiative
EU	European Union
FBR	Fast Breeder Reactor
FP	Fission Product
FPC	Fuel Performance Code
FR	Fast Reactor
Gen-IV	Generation IV
HBS	High Burnup Structure
HM	Heavy Metal
INSPYRE	Investigations Supporting MOX Fuel Licensing for ESNII Prototype Reactors
JPNM	Joint Programme on Nuclear Materials
JRC	Joint Research Centre
LAMMPS	Large-scale Atomic/Molecular Massively Parallel Simulator
LWR	Light Water Reactor
MA	Minor Actinide
MOX	Mixed-OXide
O/M	Oxygen-to-Metal ratio
PIM	Partially Ionic Model
POLIMI	Politecnico di Milano
RLS	Reflected Light Signal
rmse	root mean square error
TD	Theoretical Density

1 INTRODUCTION

Minor actinide-bearing mixed oxide fuels $(U,Pu,Am,Np)O_{2-x}$ (MA-MOX) are advanced nuclear fuels envisaged to be employed in fast breeder and transmutation reactors. Additionally, when MOX fuel is irradiated to the target high burnup for Gen-IV applications [1,2], significant quantities of fission products (FPs) and minor actinides (MAs) are formed in the fuel matrix, in solid solution and as oxide precipitates metallic inclusions. This fuel microstructure modification during irradiation directly affects the fuel thermal and mechanical properties.

Data on the thermodynamic and physical properties of MA-MOX fuels, pivotal to simulate and understand their performance under irradiation, are scarce in the current literature. This is mainly due to the difficulties in fabricating and measuring materials containing highly radioactive MA isotopes (e.g., Am-241, α-decaying). To complement experimental data, atomic scale modelling is a useful simulation technique to obtain information on the behaviour of MA-containing materials and to evaluate their physical properties.

The focus of this report is the thermal conductivity and melting (solidus) temperature of Am and Np-bearing MOX, which determine the fuel temperature profile and the safety margin to fuel melting, and impact the overall fuel performance under irradiation. The correlations developed here for MA-MOX fuels are an extension of a previous modelling activity performed in INSPYRE on U-Pu MOX fuels.

The document is structured as follows. Section 2 presents a literature review on melting temperature and thermal conductivity of MA-MOX, including both currently available data and existing correlations. Section 3 and Section 4 are dedicated to the development and assessment of original correlations for the MA-MOX melting temperature and thermal conductivity, respectively, on physical grounds and accounting for the most relevant dependencies. Conclusions and further developments are drawn in Section 5.

The content of this Deliverable is published in: A. Magni, L. Luzzi, D. Pizzocri, A. Schubert, P. Van Uffelen, A. Del Nevo, "Modelling of thermal conductivity and melting behaviour of minor actinide-MOX fuels and assessment against experimental and molecular dynamics data", Journal of Nuclear Materials 557 (2021) 153312. [3].

2 LITERATURE REVIEW ON THERMAL PROPERTIES OF MA-MOX

The majority of experimental and simulation activities on MA-MOX (mainly Am-bearing) started in the '90s, along with the development of Gen-IV reactor concepts and the related interest in the possibility of minor actinide transmutation. Although a few experimental campaigns on minor-actinide (Am, Np)-bearing fuels were performed also in the '80s-'90s (e.g., the SUPERFACT-1 irradiation experiment [4]), the available open literature works are more recent. The investigations included the impact on the MA-MOX properties not only of the MA content, but also of the Pu content, the burnup and oxygen-to-metal ratio (O/M). An overview of both data and correlations currently available in literature is provided below, focusing on the MA-MOX melting temperature in Section 2.1 and on the MA-MOX thermal conductivity in Section 2.2.

2.1 Melting temperature of MA-MOX

2.1.1 Available data

The available literature works agree that the melting temperature of mixed oxide fuels slightly decreases when the MA content increases [5–7], in addition to the degrading effect of the fuel burnup [5,8,9]. Quantitative indications about the impact of small Am and Np additions (0.016 at.%) in MOX fuels are reported by Kato *et al.*, 2011 [10], showing a decrease of the MOX melting temperature of 2–4 K. The burnup degradation effect is quantified by Konno *et al.*, showing that the decrease of the MA-MOX melting temperature is 5, 4 and 3 K per 10 GWd/t at 50, 100 and 150 GWd/t, respectively [5], a trend qualitatively confirmed by the same authors in their later work [8]. The works by Morimoto *et al.* [11] and Tanaka *et al.* [9] consider the presence of simulated fission products in the lattice of sintered MA-MOX pellets (although the representativeness of data from SIMFUELS is still to be assessed). In particular, Tanaka *et al.* analyses the burnup dependence in Am-MOX, since the considered compositions are representative of both fresh and high burnup fuel (150 and 250 GWd/t_{HM}) [9].

Among the mentioned references, only Kato *et al.*, 2008 [6] shows the impact of a varying plutonium content. The decrease of melting temperature with increasing Pu, however, is confirmed by the majority of experimental (e.g., [12–14]) and atomic scale modelling results [15,16] on MOX fuels (at least in the current ranges of interest for FR and Gen-IV applications, i.e., Pu content < 50% and 1.90 < O/M < 2.00).

The literature data exhibit significant disagreement on the dependence of MOX and MA-MOX melting temperature on the deviation from fuel stoichiometry.: According to most authors the property should decrease with decreasing O/M (in the hypo-stoichiometric range and supposedly also in the hyper-stoichiometric one [6,8,12,17]). A few recent works, however, both experimental (e.g., Kato *et al.* 2011, [10]) and using CALPHAD calculations [16,18], indicate the opposite. For example, Morimoto *et al.*, whose investigation focuses on the dependence of the melting temperature of MA-MOX with 30% Pu, 2% Am, 2% Np on the deviation from stoichiometry, indicates an unexpected decrease of the melting temperature towards fuel stoichiometry [11]. Additionally, CALPHAD calculations reported in [16,18] show a maximum melting temperature around O/M = 1.98 and not 2.00, as commonly accepted from the experimental point of view. These considerations must, however, take into account the significant uncertainty on the fuel O/M ratio upon measurement due to the oxidation of the samples during the successive laser shots of the experimental procedure [18], which is around 2% (~ 60 K) of the measurements [6,7,12,18].

2.1.2 Available correlations

Melting temperature correlations were proposed by some of the authors cited above [5,8], but rely only on their own set of experimental measurements without integrating available information from previous works. Table 1 collects the two correlations currently available for the melting temperature of mixed oxide fuels accounting for the effect of Am only, both developed by Konno *et al.* The second (2002) [8] extends the first one (1998) [5] by including the dependence on the deviation from fuel stoichiometry. Both correlations are applicable on a wide range of burnup values, i.e., the 1998 correlation up to 124 GWd/t_{HM} and the 2002 one up to 110 GWd/t_{HM}. The neptunium content effect is currently not taken into account. They do not include an explicit dependence of the melting temperature on the soluble fission products [5].

The 1998 correlation [5] is simpler in form, obtained by fitting experimental data measured on fuel samples irradiated up to 124 GWd/t_{HM} in the Japanese experimental fast reactor Joyo. Samples were then canned in tungsten capsules for melting tests. The correlation was derived applying a combined multi-variable and experimental regression analysis, assuming additivity of the various dependencies within the dataset ranges and modelling the effect of actinides (Pu and Am) according to the ideal solution model. The analyses led to a first order dependence on the Pu and Am contents, while a quadratic dependence on the fuel burnup. The 2002 correlation [8] includes all the main variables of interest, i.e., fuel burnup, stoichiometry, plutonium and americium content. The effect of Am is included in the correlation based on the ideal solution model. As for the 1998 correlation, the applied method still consists in an experimental regression analysis under the hypothesis of additive effects. The 2002 correlation is also based on a set of data from irradiation campaigns in the Joyo reactor, representative of the deviation from stoichiometry effect in the hypo-stoichiometric range. The resulting correlation features quadratic dependence on Pu content and fuel burnup, as well as mixed-effect terms.

Table 1: List of state-of-the-art melting temperature correlations, available in the open literature or employed by FPCs, for MA-MOX fuel. The dependencies included in each correlation are indicated.

Correlation	O/M	Pu content	Am content	Burnup
Konno *et al.*, 1998 [5]		X	X	X
Konno *et al.*, 2002 [8]	X	X	X	X

2.2 Thermal conductivity of MA-MOX

2.2.1 Available data

The experimental thermal conductivity of MA-MOX as a function of temperature is well described by a modelling approach based on solid-state physics theory. It includes on the one hand the lattice vibration contribution, representing the phonon–phonon interaction (Umklapp process) and the interactions with the density of defects in the lattice (which dominate at low temperatures), and on the other hand the contribution from free electrons (dominating at high temperatures) [7,10]. The thermal conductivity values measured decrease when the temperature decreases (down to a minimum value at around 1800-2000 K) [7,19–21], while their slight increase at high temperatures is indicated by atomic scale calculations [22,23] or measurements on U-Pu MOX fuels [17,24,25]. This behaviour holds for any value (in reasonable ranges) of fuel deviation from stoichiometry (i.e., O/M ratio), porosity and minor actinide (Am, Np) contents, as shown e.g., by [47]-[48], [19], and [21], respectively. The effect of plutonium content and the degradation of the thermal conductivity with burnup (during fuel irradiation) is mainly suggested by observations on U-Pu MOX rather than on MA-MOX, since each available reference on MA-

MOX analyses the effect of MAs for a fixed Pu content. Only one author provides two experimental values for irradiated MA-MOX [10], which is not sufficient to derive a burnup effect specifically representative of MA-MOX. A clear and quantitative indication of the small effect of the MA content on the fuel thermal conductivity is provided by Kato *et al.* [10]. It is reported there that the Np and Am additions to MOX caused the measured data to decrease slightly (in the lower temperature range < 1000 K), i.e., the 1.6% Am content and 1.6% Np content caused the thermal conductivity to decrease by 2.0–2.5% of the U-Pu MOX value. The variation is hence supposed to be negligibly small also in the operative temperature range of fast reactor MOX fuels [10].

In addition to experimental works, two publications are available on the calculation of the thermal conductivity of MA-MOX fuels using atomic scale methods [22,23]. Both consider stoichiometric, fully dense Am-MOX with 30 at.% Pu content, but covering wide ranges in terms of temperature (up to melting temperatures) and Am content (up to 25 at.%, hence well beyond the limit for the homogeneous recycling of MAs, typically set at 5%). In both works, the thermal conductivity obtained does not account for the electronic contribution at high temperature. Therefore, it continuously decreases when the temperature increases due to the phonon contribution, with low temperatures values higher than the experimental ones. The effect of the Am inclusion into the material lattice is slight, especially at higher temperatures, while noticeable at 500 K according to [23]. The uncertainties calculated and reported by [22] amount to approximately 20% at room temperature, decreasing with increasing temperatures.

2.2.2 Available correlations

The experimental data on MA-MOX thermal conductivity mentioned above were in most cases exploited by the same authors as a basis (fitting datasets) to propose original correlations. The correlations developed for the MA-MOX thermal conductivity, currently available in literature, are summarized in Table 2. They generally include the lattice vibration (phonon) contribution, expressing the temperature dependence in the form $(A+BT)^{-1}$ and describing well the data measured at temperatures < 1800 K [19–21]. The phonon contribution to thermal conductivity is corrected (in the A and B coefficients) for the Am content in stoichiometric Am-MOX [19], for the deviation from stoichiometry in $(U_{0.68}Pu_{0.3}Am_{0.02})O_{2\pm x}$ [20] and for both the Am and Np contents in MA-MOX [21]. Besides, Prieur *et al.* [7] modelled the thermal conductivity of MA-MOX (with up to 3.5% Am and 2% Np contents) using only a phonon term for temperatures up to 1600 K. The authors all agree on a higher impact (i.e., stronger degradation of the thermal conductivity) of Am than of Np on the thermal conductivity of MA-MOX, although the impact is smaller in percentage than that of Pu. Moreover, the MA impact proves to be represented in the A coefficient, while B can be considered independent on the MA content (both at small MA contents < 5% and also at 10% Am content as suggested by [26]).

Kato *et al.* [10] extended the modelling obtained at low temperatures based on [20,21] to high temperatures, introducing an additional electronic contribution exponential in temperature based on data from [27] (not accessible by the authors). This form of electronic contribution to thermal conductivity is also found in correlations describing LWR and FR U-Pu MOX fuels [17,28–30]. Although measurements of MA-MOX fuels irradiated in fast reactors are reported in Kato's work, they are not sufficient to represent a burnup effect in the proposed correlation, hence the correlation is only applicable to fresh MA-MOX [10]. Table 2 evidences that none of the state-of-the-art correlations include the evolution of MA-MOX thermal conductivity with fuel burnup, mainly because of the very few experimental data currently available. As a consequence, neither the impact of fission products (dissolved or precipitated), nor of radiation-induced lattice defects (by neutron or α-decay) is at present accounted for. In addition, none of the current correlations takes into account both the Pu and MA content.

In addition, the TRANSURANUS FPC [28] includes two thermal conductivity correlations, based on data measured on specific MOX fuels irradiated during the SUPERFACT-1 campaign [4]. The fuels considered are $(U,Am,Np)O_2$ with 25% Am, 25% Np contents and $(U,Np)O_2$ with 50% Np and the models depend on temperature, but not on O/M, Pu content or burnup.

Table 2: List of state-of-the-art thermal conductivity correlations available in the open literature or employed by FPCs for MA-MOX fuel. The dependencies included in each correlation are indicated.

Correlation	Temper-ature	O/M	Pu content	Am content	Np content	Porosity	Burnup
Morimoto *et al.*, 2008 [19]	X			X		X	
Morimoto *et al.*, 2008 [20]	X	X				X	
Morimoto *et al.*, 2009 [21]	X			X	X	X	
Kato *et al.*, 2011	X	X		X	X	X	
Prieur *et al.*, 2015 [7]	X						
TRANSURANUS, SUPERFACT-1 [28]	X						

3 MODELLING OF MELTING TEMPERATURE OF MA-MOX

This section presents the novel correlation for the melting temperature of minor actinide-bearing MOX fuel derived in this work. This correlation is obtained from a best fit of selected measurements, while additional CALPHAD data are kept for comparison and additional validation.

3.1 Fitting dataset

All the experimental data publicly available on the melting temperature of MA-MOX mentioned in Section 2.2.1 are collected in Table 3. The measurements concern mainly stoichiometric MA-MOX fuel, but also a few hypo-stoichiometric fuel. The fuel composition studied and the measurement technique employed are indicated in the table.

We selected as fitting dataset of our melting temperature correlation for MA-MOX fuel, covering both fresh and irradiated material, a restricted number of data points. For fresh MA-MOX, we considered the data obtained by Kato *et al.* [6], Prieur *et al.* [7] and by Fouquet-Métivier via recent measurements performed at JRC-Karlsruhe [18]. Among Kato *et al.* measurements [6], only those performed in rhenium inner capsules (sealed into outer tungsten capsules) have been selected, due to the confirmed strong contamination by W of the melted fuel material, which heavily affects the melting temperature measured [38], [40]. These data all correspond to stoichiometric MA-MOX, bearing both Am and Np. Data on hypo-stoichiometric are instead provided by Prieur (Am, Np-MOX) and Fouquet-Métivier (Am-MOX). The measurements by Fouquet-Métivier on hyper-stoichiometric fuel are excluded since beyond the scope of the present analysis, focused on the hypo-stoichiometric range.

Table 3: Literature studies of MA-MOX melting temperature, with details about the fuel material and the experimental technique employed.

Reference	Fuel studied	Experimental technique	Selection
Konno *et al.*, 1998 [5]	Fresh and irradiated Am-MOX: burnup = 0 - 124 GWd/t_{HM}, O/M = 1.95 - 1.98, Pu content ~ 30 mol%, Am content = 0.04 and 0.9 mol%.	Thermal arrest technique on samples in W capsules.	Validation
Konno *et al.*, 2002 [8]	Irradiated Am-MOX: burnup = 8.2 - 110.9 GWd/t_{HM}, O/M = 1.98, Pu content = 17.5 mol%, Am content = 0.13 mol%.	Thermal arrest technique on samples in W capsules.	Fit
Morimoto *et al.*, 2005 [11]	Fresh MA-MOX (Sample 1): $(U_{0.66}\ Pu_{0.30}\ Am_{0.02}\ Np_{0.02})O_{2-x}$, x=0.012, 0.037.	Thermal Arrest technique and analysis of pyrometer thermograms.	Validation
Kato *et al.*, 2008 (b) [6]	Fresh Am-MOX, O/M = 1.922 - 2.000, Pu content = 11.7 - 60.0 mol%, Am content = 0.3 - 3.3 mol%.	Sample heating in a Re or W capsule, analysis of pyrometer thermograms.	Fit
Kato *et al.*, 2011 [10]	Irradiated, hypo-stoichiometric MA-MOX: $(U_{0.668}\ Pu_{0.3}\ Np_{0.016}\ Am_{0.016})O_{2-x}$, x = 0.017, 0.043, burnup = 0.082 GWd/t_{HM}.	Short irradiation tests performed in the Joyo fast reactor [32–35]. Samples in rhenium inner capsule, model for solidus/liquidus temperature (based on ideal solid solution) employed for interpretation of measurements.	Fit
Tanaka *et al.*, 2012 [9]	Irradiated Am-MOX fuel containing simulated fission products: $(U_{0.665}\ Pu_{0.29}\ Am_{0.03}\ FP_{0.015})O_2$, bu = 150 GWd/$t_{HM}$.	Thermal arrest method on crushed pellet loaded into a Re inner capsule (W outer capsule).	Validation
Prieur *et al.*, 2015 [7]	Fresh, hypo-stoichiometric MA-MOX: $(U_{0.74}\ Pu_{0.22}\ Am_z\ Np_w)O_{2-x}$, (x, z, w) = (0.01, 0.02, 0.02) and (0.02, 0.035, 0.005).	Laser heating and analysis of pyrometer thermograms: onset of melting detected by the appearance of vibrations in the signal of a probe laser reflected by the sample surface (RLS technique).	Fit
Fouquet-Métivier *et al.*, 2020 [18]	Fresh, hypo-/hyper-stoichiometric Am-MOX: Pu content = 28%, Am content = 1 - 2%, O/M = 1.98 - 2.05.	Laser-flash tests on samples in a self-crucible setup: 8 successive shots on same sample, recording of pyrometer thermograms.	Fit

Data on MA-MOX by Morimoto *et al.*, including the simulated effect of fission products [11], are excluded because of the behaviour of melting temperature as a function of deviation from stoichiometry (decreasing with decreasing off-stoichiometry). This is opposite to what indicated by the majority of experimental and modelling works currently available in literature, concerning various types of oxide

fuels [8,17,28,31]. The suitable data about irradiated MA-MOX are those provided by the second study of Konno *et al.* [8], already considered in [17,25] and corresponding to fuel irradiated up to high burnup (~ 110 GWd/t_{HM}), and by Kato *et al.* [10], where fuel burnup is very low (< 1%). The first data on irradiated MA-MOX by Konno *et al.* [5] are not used here since the measurements performed in W capsules led to sensibly lower measured melting points and also, the actual O/M values of the irradiated fuel samples are not reported. The single data point at very high burnup (150 GWd/t_{HM}) and 29% Pu content available from Tanaka *et al.* [9] is kept for additional comparison and considerations, since it includes the effect of simulated fission products.

The selected data on both fresh and irradiated MA-MOX fuels (from Table 3) correspond to low MA contents (up to 3.5% Am content and 2% Np content, with the majority of data on Am-MOX) and to Pu contents in line with values of interest for FR and Gen-IV applications (between 16% and 60% Pu).

3.2 Development of a correlation for MA-MOX melting temperature

The correlation proposed for the melting (solidus) temperature of MA-MOX fuel relies on the same modelling strategy and hypotheses as the already published correlation for U-Pu MOX fuels [17,25]. The strategy consists in a two-steps model development. First a correlation suitable for fresh MA-MOX ($T_{m,0}$) is derived by fitting the selected fresh MA-MOX experimental data. Then, a correlation describing the melting temperature evolution with fuel burnup is obtained by including $T_{m,0}$ in a formulation fitted on the data measured on irradiated fuel. A linear dependency on each parameter known to affect (decrease) the melting temperature is assumed and the effects are considered to be independent (i.e., additive to each other) to keep a simple modelling, especially in light of the limited set of available experimental data. The correlation for fresh MOX [17,25] is extended with the inclusion of the Am and Np effects (supposedly acting as the Pu content), as follows:

$$T_{m,0}(x,[Pu],[Am],[Np]) = T_{m,UO_2} - \gamma_x\, x - \gamma_{Pu}\,[Pu] - \gamma_{Am}\,[Am] - \gamma_{Np}\,[Np] \quad (1)$$

Where,

- T_{m,UO_2} is the melting temperature of fresh stoichiometric UO_2, i.e., 3147 K according to recent and reliable experimental measurements by Manara *et al.* [36] and recommended by the ESNII+ Catalogue on MOX properties [37]
- $[Pu]$, $[Am]$, $[Np]$ are the plutonium, americium and neptunium contents, respectively
- x is the deviation from fuel stoichiometry
- $\gamma_x, \gamma_{Pu}, \gamma_{Am}, \gamma_{Np}$ are the regressors associated to each effect, to be fitted on the selected fresh MA-MOX melting temperature data.

The multi-dimensional fit is performed using both MATLAB tools [38] and the R software [39] to obtain the regressor values, the related p-values, the confidence intervals and the fit residuals. The significance of each MA-related regressor of the supposed functional form is evaluated considering the associated p-value as figure of merit, compared to a threshold p-value of 5% (corresponding to a 95% confidence on the significance of a regressor). A regressor is kept in the final correlation if the associated p-value is below 5%, otherwise it is rejected as statistically insignificant, i.e., not well represented by the fitting dataset. The analysis reveals the significance of the Am effect but excludes the Np effect, based on the fitting dataset. The p-value associated to the Np-dependent contribution is always high (~ 71%), even when tested on sub-sets of data representing only the Np dependence. The amount of available data on fuel with Np content is very limited (four data points in total), hence the Np effect on the MOX melting

temperature cannot be well represented and justified. As a result, the novel correlation for the melting temperature of fresh MA-MOX is established as follows:

$$T_{m,0}(x,[Pu],[Am]) = T_{m,UO_2} - \gamma_x\, x - \gamma_{Pu}\,[Pu] - \gamma_{Am}\,[Am] \quad (2)$$

The best fit of Eq. 2 over the set of fresh MA-MOX melting temperature data (from Table 3) yields the regressor values shown in Table 4. The values of the γ_x and γ_{Pu} coefficients are kept as in the MOX correlation [17,25], while γ_{Am} corresponds to the best fit of the experimental data on fresh MA-MOX fuel. The fit coefficient values reported in Table 4 hold for T_{m,UO_2} expressed in K, $[Pu]$ and $[Am]$ expressed in at./ and $T_{m,0}$ in K. The analysis of the trends of the fit residuals, also considering the Am-dependent term, shows that all the fit residuals are randomly distributed if plotted against x, $[Pu]$ or $[Am]$. Therefore, there is no need to introduce higher order or terms of mixed dependencies (included instead in the correlation by Konno *et al.* [8]).

Table 4: Coefficients of the $T_{m,0}(x,[Pu],[Am])$ correlation (Eq. 2). The values of γ_x and γ_{Pu} are kept equal to those used for fresh MOX fuel [17,25].

Regressor	Units	Estimate	Std. Error
$\boldsymbol{\gamma_x}$	K	1014.15	253.57
$\boldsymbol{\gamma_{Pu}}$	K/at./	364.85	13.96
$\boldsymbol{\gamma_{Am}}$	K/at./	329.5	223.2

The expression for the melting temperature of fresh MA-MOX, $T_{m,0}(x,[Pu],[Am])$ (Eq. 2, with regressor values in Table 4) is then used as a basis for a burnup dependent formulation consisting in an exponential, asymptotic decrease of melting temperature with burnup, as for the melting temperature of irradiated MOX fuels [17,25]. This formulation accounts for the continuous build-up of defects and fission products shown by experimental observations and results of atomic scale calculations (e.g., [5], [15]). Hence, the formulation chosen for the complete correlation, extended to irradiated MA-MOX and to be fitted to the selected burnup dependent data [8,10], reads

$$T_m(x,[Pu],[Am],bu) = T_{m,inf} + (T_{m,0} - T_{m,inf}) \cdot e^{-\frac{bu}{\delta}} \quad (3)$$

Where,

- bu is the fuel burnup in GWd/t_{HM}
- $T_{m,0} = T_{m,0}(x,[Pu],[Am])$ is the melting temperature of the fresh fuel according to Eq. 2
- $T_{m,inf}$ and δ are the correlation parameters to be fitted on the set of irradiated MA-MOX melting temperature data.

This formulation is consistent with the MOX fuel correlation [17,25] for zero Am and Np contents. Fitting the functional form of Eq. 3 to the irradiated MA-MOX data [8,10] leads to the fit regressor values reported in Table 5. The values of the coefficients $T_{m,inf}$ and δ only slightly differ to the values reported for MOX fuels [17,25] due to the limited number of additional measurements on MA-MOX available.

Table 5: Results of the best fit of the $T_m(x,[Pu],[Am],bu)$ correlation (Eq. 3) on the set of selected experimental data on the melting temperature of irradiated MA-MOX [8,10].

Regressor	Units	Estimate	Std. Error
$\boldsymbol{T_{m,inf}}$	K	2964.94	34.62
$\boldsymbol{\delta}$	GWd/t_{HM}	41.01	24.25

The comparison between the results yielded by the correlation developed and the experimental data included in the fitting dataset (Section 3.1), is shown in Figure 1. The agreement between the predictions and the experimental data confirms the quality of the fit, both concerning fresh and irradiated MA-MOX. Most of the predictions lie within the 1% deviation band from the perfect agreement (i.e., maximum ~ 30 K deviation from the measurements, corresponding to the best experimental uncertainty at the state of the art [6,13,40–42]). The entire cloud of points in Figure 1 is included in the 2% deviation band, in line with the typical experimental uncertainty reported in literature.

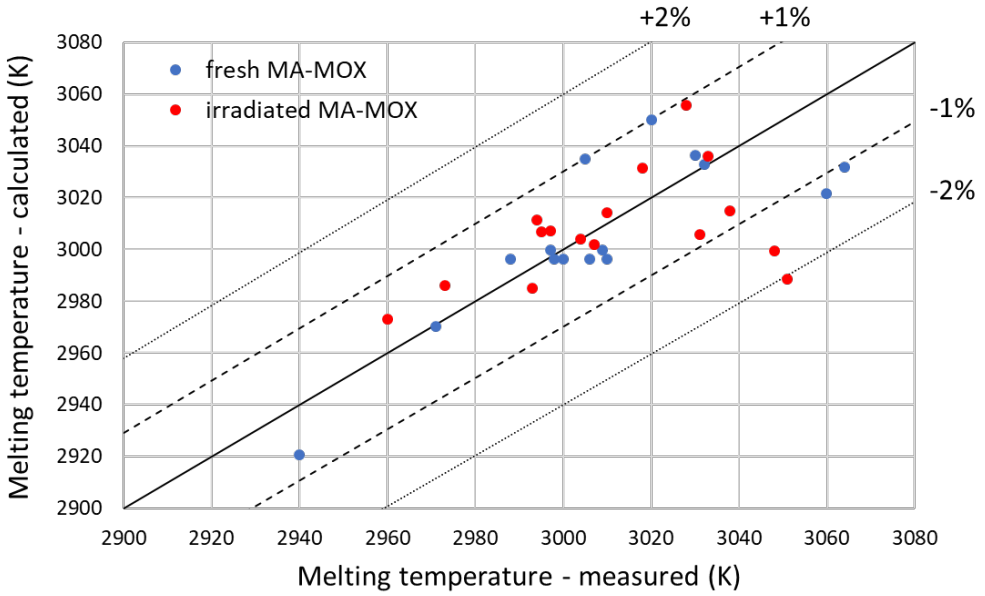

Figure 1: Comparison of the experimental data of both fresh and irradiated MA-MOX melting temperature (Table 3) and the results of the correlation developed in this work (Eq. 2 and 3 with coefficients in Tables 4 and 5).

Table 6 reports the root mean square error of the correlation developed and Konno's ones [5,8] on the entire set of available experimental data, both on fresh and irradiated MA-MOX fuel (Section 3.1). The error of the novel correlation developed in this work is less than half the error of the other two literature correlations for MA-MOX [5,8].

Table 6: Root mean square error of the correlation for the MA-MOX melting temperature developed in this work, compared to literature correlations for MA-MOX fuel, over the fitting dataset including both fresh and irradiated MA-MOX [6–8,10,18].

	Konno *et al.* [5]	Konno *et al.* [8]	This work
Root mean square error (rmse)	0.017	0.016	0.007

Figure 2 compares the behaviour of the correlation developed for the MA-MOX melting temperature, as a function of burnup and Am content, with the two state-of-the-art correlations available in the open literature [5,8]. In terms of fuel burnup, the novel correlation exhibits an exponential, asymptotic decreasing trend, leading to higher predicted melting temperatures at high burnup. This reflects the characteristics of the fuel microstructure at high burnup, when the formation of a highly porous HBS in the low temperature fuel region determines a reduction of the FP concentration in the lattice [43–45]. This process, together with a large fractional release of fission products occurring in FBR MOX fuels at high temperature, causes a reduced rate of decrease of the fuel melting temperature. The results of the correlations at high burnup are compared with the only experimental measurement available, by

Tanaka *et al.* [9] at 150 GWd/t_{HM}. Although the novel correlation proves to be the farthest from this single experimental point, the deviation (~ 50 K) is still in line with the state-of-the-art experimental uncertainties on the mixed oxide melting temperature (30 - 60 K) [17,25]. Moreover, this experimental point accounts for the degrading effect of simulated FPs on the melting temperature, which is not explicitly represented by the proposed correlation (the effect is included in the burnup dependence). The novel correlation, fitted on a wider set of experimental data, features a smaller dependence on the Am content than that of the Konno's correlations, which is fitted only on own data [5,8].

The ranges of applicability of the novel correlation proposed for the melting temperature of MA-MOX fuels are consistent with the ranges covered by the fitted experimental data [6–8,10,18]:

- Deviation from stoichiometry, x: [0, 0.06] (hypo-stoichiometry)
- Plutonium content, [Pu]: [0, 50] at.%
- Americium content, [Am]: [0, 3.5] at.%
- Burnup, bu: extended to [0, 150] GWd/t_{HM}.

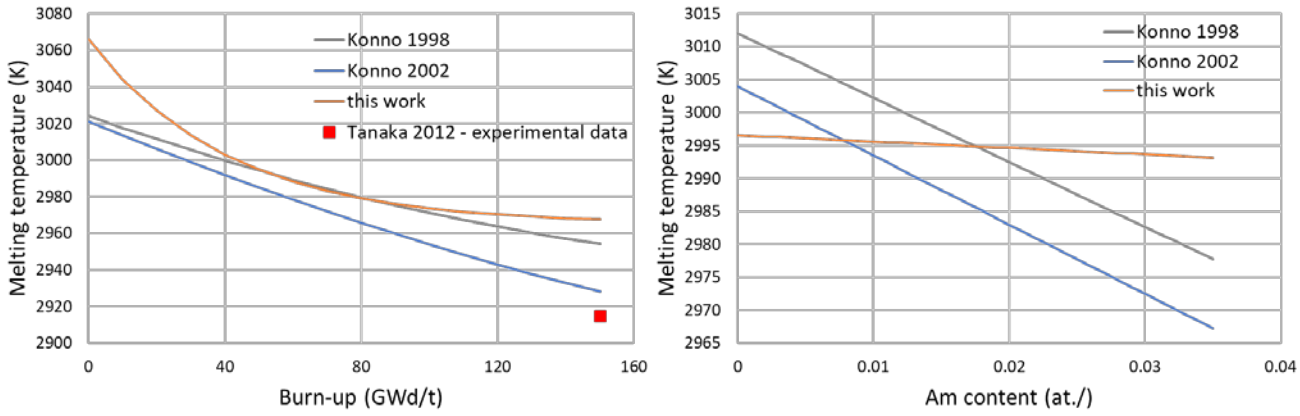

Figure 2: Behaviour of the novel MA-MOX melting temperature correlation (orange line), as a function of fuel burnup (left) and Am content (right), compared to the two correlations for MA-MOX from state-of-the-art literature [5,8]. Both plots refer to hypo-stoichiometric MA-MOX with x = 0.002 and Pu content = 20 at.%, while Am content = 1.8 at.% in the left plot (to reproduce the experimental point from [9]), and burnup = 50 GWd/t_{HM} in the right plot.

Since the MA-MOX correlation is an extension of the MOX fuel correlation and includes the application to U-Pu MOX, the range of validity in terms of deviation from stoichiometry is mainly dictated by the experimental data on U-Pu MOX [17,25]. The range in plutonium content is limited to 50 at.%, due to contradictory results available in literature for the melting temperature of very high Pu content-MOX [15,16,41]. The correlation can be deemed applicable to high burnup (above the limit of the experimental data fitted [8]) thanks to its good performance compared to the value at 150 GWd/t_{HM} provided by [9].

4 MODELLING OF THERMAL CONDUCTIVITY OF MA-MOX

This section presents the correlation developed for the thermal conductivity of minor actinide-bearing MOX fuel. The correlation is obtained from a best fit of the selected experimental data, while results of atomic scale calculations are kept for comparison and additional validation.

4.1 Fitting dataset

The accessible literature works providing experimental data or atomic scale calculations of the thermal conductivity of MA-MOX are collected in Table 7. The data concern mainly stoichiometric but also hypo-stoichiometric MA-MOX fuel. The fuel composition studied and the measurement / modelling technique employed are described.

Considering the limited amount of information available in the open literature, all the experimental works listed in Table 7 have been deemed valid. Most of them provide measurements on fresh MA-MOX fuels, namely Morimoto's works [19–21], on stoichiometric Am-MOX, hypo-stoichiometric Am-MOX and stoichiometric Np-MOX, respectively; Prieur's data on both Am and Np-bearing hypo-stoichiometric MOX fuels [7]; the recent Yokohama's data on stoichiometric MOX with higher Am content (10%) [26]. Only one literature work is currently available on irradiated MA-MOX, by Kato *et al.* [10], providing just two data points with two limitations, besides the low MA content: a single, low temperature of measurement (1273 K) and a very low fuel burnup (< 1%), from very short irradiation campaigns performed in the Joyo fast reactor.

All the measurements correspond to a temperature range from 300 K up to 1800 K, deviation from fuel stoichiometry up to 0.085 (in the hypo-stoichiometric range), 30% Pu content (apart from Prieur's measurements, at 22% Pu content [7]), Am content up to 10%, Np content up to 12%, porosity up to ~ 16% TD (although most of the data are normalized to 100% TD), fresh fuel or at very low burnup [10] (consistent with reactor start-up situations).

Table 7 lists two set of results of atomic scale calculations of the thermal conductivity of Am-MOX, namely by Kurosaki *et al.* [22] and by Li *et al.* [23]. These data are not part of the fitting dataset for the correlation, but were used to compare the correlation results to independent data.

4.2 Development of a correlation for MA-MOX thermal conductivity

Similarly to the correlation developed for the thermal conductivity for U-Pu MOX fuels [17,25], the model development for MA-MOX is performed in two steps. First, a correlation for fresh MA-MOX thermal conductivity (k_0) is derived based on the selected fresh MA-MOX experimental data. Then, a correlation describing the evolution during fuel irradiation is obtained by including k_0 in a burnup dependent formulation, fitted on available data measured on irradiated fuel.

Table 7: Literature studies of MA-MOX thermal conductivity (experimental and atomic scale calculations), with details about the fuel material and the experimental/modelling technique employed.

Reference	Fuel studied	Experimental/modelling technique
Kurosaki *et al.*, 2006 [22]	Atomic scale calculations on fresh, stoichiometric Am-MOX: $(U_{0.7-z}\ Pu_{0.3}\ Am_z)O_2$, z = 0, 0.016, 0.03, 0.05, 0.1, 0.15. T = 300 - 2500 K, density = 100% TD.	Ions arranged in a CaF_2 type crystal structure. Calculations based on MXDORTO, employing the semi-empirical two-body potential function by Ida [46]. Thermal conductivity calculated using the Green-Kubo relation.
Morimoto *et al.*, 2008 [19]	Fresh, stoichiometric Am-MOX: $(U_{0.7-z}\ Pu_{0.3}\ Am_z)O_2$, z = 0.007, 0.022, 0.03. T = 873 - 1673K, density = 84.3% - 100% TD.	Laser-flash method for the simultaneous measurement of thermal diffusivity and specific heat capacity (calorimeter in the sample position).
Morimoto *et al.*, 2008 [20]	Fresh, hypo-stoichiometric Am-MOX: $(U_{0.678}\ Pu_{0.3}\ Am_{0.022})O_{2-x}$, x = 0.001 - 0.085. T = 870 - 1773 K, density = 100% TD.	Laser-flash method for the simultaneous measurement of thermal diffusivity and specific heat capacity (calorimeter in the sample position).
Morimoto *et al.*, 2009 [21]	Fresh, stoichiometric Np-MOX: $(U_{0.7-z}\ Pu_{0.3}\ Np_w)O_2$, w = 0.06, 0.12. T = 870 - 1800 K, density = 93%, 94.1% TD.	Laser-flash method for the simultaneous measurement of thermal diffusivity and specific heat capacity (calorimeter in the sample position).
Kato *et al.*, 2011 [10]	Irradiated, hypo-stoich. MA-MOX: $(U_{0.668}\ Pu_{0.3}\ Np_{0.016}\ Am_{0.016})O_{2-x}$ x = 0.017, 0.043. T = 1273 K, density = 93% TD, burnup = 0.082 GWd/t_{HM}.	Short irradiation tests performed in the Joyo fast reactor [32–35]. Thermal conductivity evaluated from irradiated samples characteristics, according to [19–21].
Prieur *et al.*, 2015 [7]	Fresh, hypo-stoichiometric MA-MOX: $(U_{0.74}\ Pu_{0.22}\ Am_z\ Np_w)O_{2-x}$, (x, z, w) = (0.01, 0.02, 0.02) and (0.02, 0.035, 0.005). T = 540 - 1615 K, density = 94.8%, 94.6% TD.	Thermal diffusivity measurement: shielded laser-flash device, temperature perturbation on the opposite surface of the sample recorded with a pyrometer. Thermal conductivity calculated via heat capacity (Neumann-Kopp's law) and density (from measured lattice parameter, accounting for porosity).
Li *et al.*, 2016 [23]	Atomic scale calculations on fresh, stoichiometric Am-MOX: $(U_{0.7-z}\ Pu_{0.3}\ Am_z)O_2$, z = 0, 0.03, 0.05, 0.1, 0.15, 0.2, 0.25. T = 500 - 3000 K, density = 100% TD.	Equilibrium atomic scale simulations with LAMMPS program, on 3 different fluorite unit cells: 4×4×4, 5×5×5 and 8×8×8 unit cells. BMH interatomic potential with PIM. Thermal conductivity calculated according to Green-Kubo relation.
Yokohama *et al.*, 2020 [26]	Fresh, stoichiometric Am-MOX: Pu content = 30%, Am content = 10%, T = 300 - 1500 K, density = 100% TD.	Thermal diffusivity measurement with laser-flash method, after heat treatment at 1473 K (to recover lattice defects induced by self-irradiation during long-term storage, and to adjust the O/M ratio of the sample to 2.00). Thermal conductivity calculated via heat capacity (Kopp's law) and density (measured).

The modelling adopted, justified by the small effect of minor actinides inclusions on the MOX thermal conductivity [10], consists in keeping formulation used for the MOX thermal conductivity [17,25]. It is a physically grounded expression $k_0\,(T, x, [Pu], p)$, including two temperature-dependent contributions (lattice vibration (phonons) and electronic, dominant at low and high temperature, respectively), corrected with the inclusion of plutonium and stoichiometry-dependent terms in the lattice contribution, and of a porosity factor. It includes all the relevant dependencies for the MOX thermal conductivity and is therefore deemed as the best starting point to derive an extended correlation suitable for MA-MOX. Under the assumption that the coefficients of the MOX correlation [17,25] hold for the MA-MOX thermal conductivity, the additional dependencies on the Am and Np contents are introduced as modifications to the *A* and *B* terms of the lattice vibration contribution, similarly to effect of the Pu content and of the deviation from stoichiometry. Hence, the functional form of the thermal conductivity correlation for fresh MA-MOX is

$$k_0(T, x, [Pu], [Am], [Np], p) = \left(\frac{1}{A + BT} + \frac{D}{T^2} e^{-\frac{E}{T}}\right)(1 - p)^{2.5} \tag{4}$$

With:

- $A = A_0 + A_x \cdot x + A_{Pu}[Pu] + A_{Am}[Am] + A_{Np}[Np]$, $B = B_0 + B_{Pu}[Pu] + B_{Am}[Am] + B_{Np}[Np]$, i.e., the Am and Np content effects are blindly introduced both in the *A* and *B* terms, in absence of precise indications available in literature [7,10,21]
- A_0, A_x, A_{Pu}, B_0, B_{Pu}, D, E are the coefficients already fitted on MOX fuel data for the effects of temperature, Pu content and deviation from stoichiometry [17,25]
- A_{Am}, A_{Np}, B_{Am} and B_{Np} are the additional correlation coefficients for the MA effects, to be fitted on the set of fresh MA-MOX experimental data.

The validity for MA-MOX of the classical modelling of the phonon transport contribution to thermal conductivity (i.e., the lattice vibration term $(A+BT)^{-1}$) was confirmed in [7] up to about 1400 K.

Following the same assessment approach adopted for the fresh MOX correlation [17,25], the statistical significance of the original contributions to the correlation (depending on the chosen fitting dataset) is evaluated by means of a statistical analysis based on the regressor p-values, performed again using R and MATLAB tools [38,39] and still assuming a threshold p-value of 5%. The initial values of the coefficients, required by the non-linear fit iterations searching for convergence, were fixed equal to the corresponding values employed by existing correlations [10,19,21]. Moreover, the stability of the fit results and their independence on the initial values was tested, within reasonable ranges of the initial values. The correlation is then verified against the entire set of available experimental data (Section 4.1) as well as against sub-sets composed by data corresponding to a dependence on only the Am or Np content. The aim of these partial fits is to achieve higher confidence on the significance of each correlation regressor, focusing only on the p-values.

The resulting p-values confirm the inclusion of the four supposed MA-related regressors (i.e., A_{Am}, A_{Np}, B_{Am}, B_{Np}) in the correlation, with the best p-value associated to A_{Am} (< 1%, while the others are reasonably closer to the 5% threshold). The fit of the formulation of Eq. 4, statistically assessed on the set of fresh MA-MOX experimental data of Table 7, leads to the coefficients of Table 8. The final regressor values were obtained imposing their positivity as a constraint in order to guarantee the degradation of the MA-MOX thermal conductivity with increasing Am and Np contents, consistently with the experimental observations (Table 7) and with theoretical considerations about phonon interactions with lattice defects [21,47,48]. The regressor values reported in Table 8 are valid for americium and neptunium concentrations ($[Am]$, $[Np]$) expressed in atomic fraction; the thermal conductivity k_0 (Eq. 4) is calculated in W/(m·K).

Table 8: Results of the fit of the statistically assessed $k_0(T, x, [Pu], [Am], [Np], p)$ correlation (Eq. 4) on the set of available experimental data on fresh MA-MOX thermal conductivity [7,19–21,26], for what concerns the MA-related regressors. The other coefficients of Eq. 4 are assumed equal to their values holding for U-Pu MOX fuel [17,25].

Regressor	Units	Estimate	Std. Error
$\mathbf{A_{Am}}$	m·K/W	0.596	0.377
$\mathbf{A_{Np}}$	m·K/W	$2.22\ 10^{-14}$	-
$\mathbf{B_{Am}}$	m/W	$5.47\ 10^{-4}$	$4.16\ 10^{-4}$
$\mathbf{B_{Np}}$	m/W	$2.48\ 10^{-14}$	-

The main effect of the Am content on the fresh MA-MOX thermal conductivity can be seen from Table 8, while the Np content proves completely negligible. In particular, the value of coefficient A_{Am} is dominant (among the effects of MAs on thermal conductivity) and in line with the value obtained by previous literature works [10,19,21]. This can be explained considering the α-activity of Am-241, which produces more lattice defects in the fuel material lattice, yielding a lower thermal conductivity of Am-MOX samples compared to U-Pu MOX or Np-MOX [7]. Furthermore, the difference in local stoichiometry / oxygen potential induced by Am or Np, which is reported by [7], may contribute to a different (local) thermal conductivity. This is mainly due to the presence of Am(III), which induces vacancies in the Am-MOX material and therefore a slight reduction in the thermal conductivity of Am-MOX.

On the contrary, little experimental information is available about Np-bearing MOX and only for low Np contents. The effect of Np concentration obtained here could be further investigated when additional data will become available. The values of A_{Am} and B_{Am} yield effects in the lattice vibration contribution $(A+BT)^{-1}$ (i.e., A_{Am}·[Am] and B_{Am}·[Am] ·T) that are compatible with the orders of magnitude of A and B in MOX [17,25]. Moreover, the dependencies on MAs are stronger in A than in B. This is consistent with previous experimental findings showing a B value that can be assumed as constant or independent from the MA content [10,19–21], and in line with theoretical considerations since the A term represent the interaction of phonons with lattice imperfections (e.g., defects, impurities).

To account for the burnup effect on the MA-MOX thermal conductivity, the model is based on an exponential, asymptotic degradation of the thermal conductivity with fuel burnup (k, Eq. 5), consistently with what already proposed for MOX fuels [17,25]. This modelling is physically-grounded since the accumulation of fission products and point defects in the material lattice with increasing burnup increases the phonon scattering effect, up to lattice saturation represented by the asymptotic thermal conductivity value and accounting for thermal recovery processes, as explained in [17,25]. Moreover, the scarce amount of data available on irradiated MA-MOX [10] supports the choice of relying on the same formulation as for the irradiated MOX thermal conductivity.

Hence, the complete correlation extended to account for the MA content in MOX fuels and for the fuel burnup reads

$$k(T, x, [Pu], [Am], [Np], p, bu) = k_{inf} + (k_0 - k_{inf}) \cdot e^{-\frac{bu}{\varphi}} \quad (5)$$

Where,

- $k_0 = k_0(T, x, [Pu], [Am], [Np], p)$ is the thermal conductivity of fresh MA-MOX calculated using Eq. 4 (employing the coefficient values collected in Table)
- bu is the fuel burnup in GWd/t_{HM}
- k_{inf} is the asymptotic thermal conductivity at high burnup
- φ is a correlation coefficient to be fitted on the irradiated fuel data.

Considering the current lack of data on irradiated MA-MOX, all the accessible experimental data about both FR MOX and MA-MOX fuels were used as fitting dataset. Hence, the Yamamoto *et al.* data on MOX at low and moderate burnup ([49], open literature) and the measurements on NESTOR-3 FR MOX fuel at high burnup ([50], performed during the ESNII+ EU Project), already considered in [17,25], are complemented by the only two available data points concerning irradiated MA-MOX (at very low burnup, [10]). The considerations leading to the best value for k_{inf}, based on MOX fuel experimental information [17,25], [1,2], are deemed valid for MA-MOX, since the values of thermal conductivity reported by [10] are compatible with the result for MOX fuels. Based on this value of k_{inf}, the best fit of the considered dataset leads to the same value for the coefficient φ, which is reasonable considering the current predominance of the MOX data over the MA-MOX ones.

The formulation of Eq. 5 is applicable to MOX fuel by setting Am and Np contents to zero. The burnup related coefficients, whose values correspond to those for MOX fuels, are collected in Table 9.

Table 9: Results of the best fit of the $k(T, x, [Pu], [Am], [Np], p, bu)$ correlation (Eq. 5) on the set of available experimental data on the thermal conductivity of irradiated MOX and MA-MOX [10,49,50].

Regressor	Units	Estimate	Std. Error
$\mathbf{k_{inf}}$	W/(m·K)	1.755	-
$\boldsymbol{\varphi}$	GWd/t_{HM}	128.75	8.59

The comparison between the results of the correlation and the available MA-MOX experimental data (Table 7), considered as fitting dataset, is shown in Figures 3 and 4, in terms of temperature dependence and validation plot, respectively.

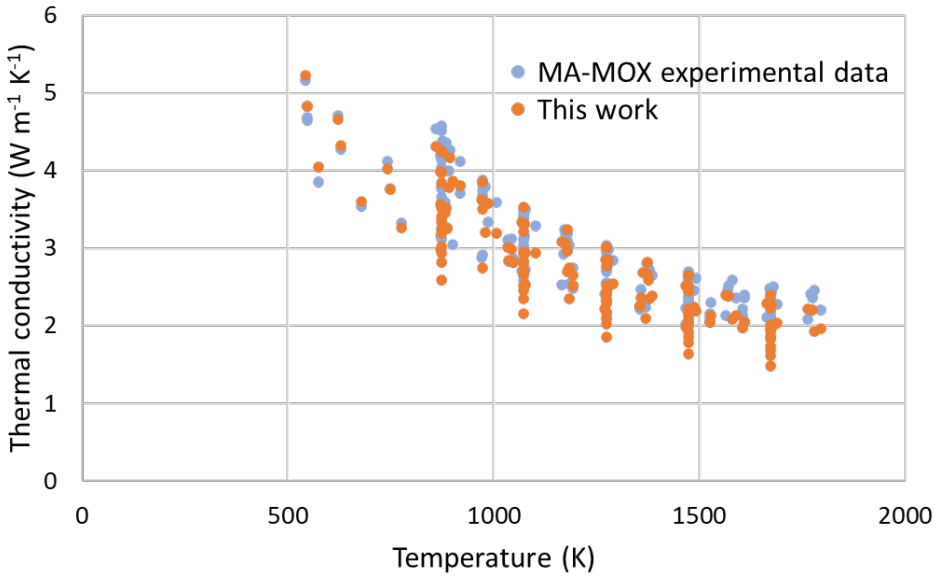

Figure 3: Temperature dependence of the MA-MOX thermal conductivity experimental data (light blue dots, Table 7), compared to the corresponding predictions provided by the novel correlation developed on this work (orange dots, Eq. 4 and 5 with coefficients in Tables 9 and 10).

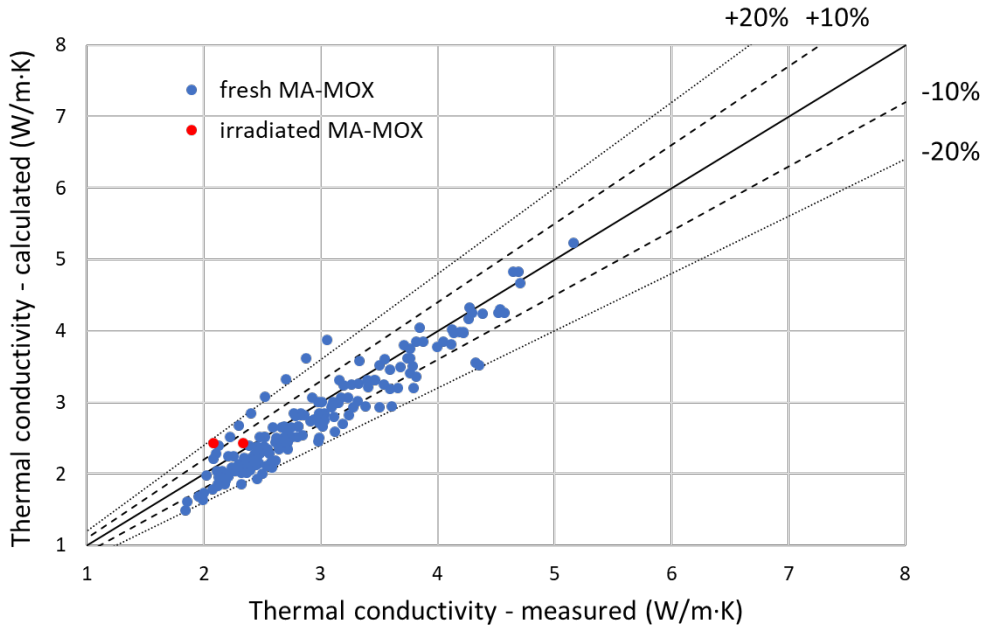

Figure 4: Comparison of the experimental data of both fresh and irradiated MA-MOX thermal conductivity (Table 7) and the results of the correlation developed in this work (Eq. 4 and 5 with coefficients in Tables 8 and 9).

The agreement between the predictions and the experimental data confirms the quality of the fit, both at low and high temperatures. A light overestimation of the data is observed at low temperatures (below 700 K) and a slight underestimation is seen at higher temperatures, where more data are available. Figure 4 includes the side-diagonals corresponding to the typical experimental uncertainties reported in literature, i.e., between 10 and 20 % of the measured values [30,40,49–52] (no specific indications on the uncertainties on the measured MA-MOX thermal conductivity are reported by the authors [7,10,19–21,26]. The only series of points outside the 20% deviation band in Figure 4 correspond to data from [21] measured on samples with higher deviation from stoichiometry (i.e.,~ 0.04, which is the limit of the applicability range of the correlation). The novel correlation therefore proves suitable to simulate the thermal conductivity of low burnup MA-MOX fuel [10].

Table 10 reports the root mean square error of the novel correlation on the entire set of MA-MOX thermal conductivity experimental data (concerning both fresh and irradiated MA-MOX, Section 4.1), compared to the rmse of three literature correlations considered for comparison [10,19,21]. The average error associated to the novel correlation is small and comparable with the rmse obtained with the correlations by Morimoto and Kato [10,19,21]. The novel correlation can be therefore considered satisfactory.

Table 10: Root mean square error of the correlation for the MA-MOX thermal conductivity developed in this work, compared to literature correlations for MA-MOX fuel, over the fitting dataset including both fresh and irradiated MA-MOX [7,10,19–21,26].

	Morimoto *et al.*, 2008 [19]	**Morimoto *et al.*, 2009** [21]	**Kato *et al.*, 2011** [10]	**This work**
Root mean square error (rmse)	0.08	0.12	0.07	0.10

The ranges of applicability of the correlation developed for the thermal conductivity of MA-MOX, mainly correspond to the ranges covered by the available experimental data and are:

- Temperature, T: [500, 2700] K
- Deviation from stoichiometry, x: extended to [0, 0.05] (hypo-stoichiometry)
- Plutonium content, [Pu]: [0, 45] at.%
- Americium content, [Am]: [0, 10] at.%
- Neptunium content, [Np]: [0, 12] at.%
- Porosity, p: extended to [0, 10] %TD
- Burnup, bu: [0, 130] GWd/t_{HM}.

The applicability of the correlation to high temperatures, plutonium contents and burnup levels is guaranteed by the available experimental data on MOX fuels [17,25]. The predictions at higher deviations from fuel stoichiometry (above 0.05) and higher porosities (above 10% TD) are not deemed reliable, due to high deviations from the measured thermal conductivity values. Data assimilation techniques [53] could be envisaged for a progressive upgrade of the correlation and further extension of its ranges of applicability, as soon as more and representative experimental results on MOX and MA-MOX fuels for FR and transmutation applications become available.

The novel MA-MOX thermal conductivity correlation was compared to the results of atomic scale calculations available in the literature [22,23]. The results of this assessment are shown in Figure 5, including the deviation bands corresponding to the typical experimental uncertainties (i.e., between 10 and 20% of the measured data) [17,25].

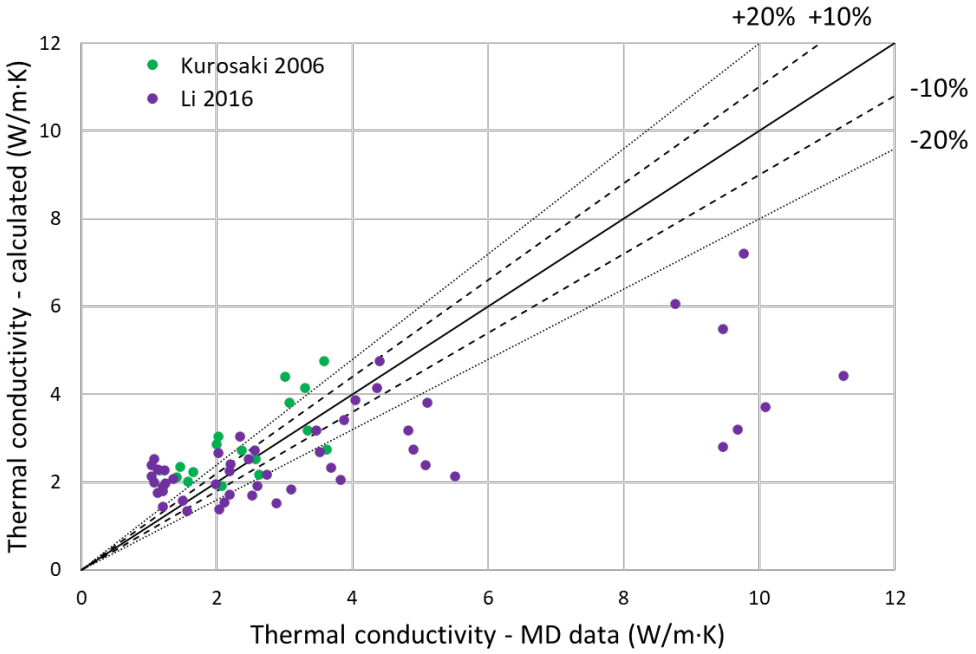

Figure 5: Comparison between the atomic scale data on MA-MOX fuel thermal conductivity ([22,23], Table 7) and the corresponding predictions given by the correlation developed in this work (Eq. 4 and 5 with coefficients in Tables 8 and 9).

A reasonable agreement between the results of the correlation and the atomic scale calculations is observed at low thermal conductivity values (1 – 4.5 W m^{-1} K^{-1}). This is true especially considering the uncertainties in the atomic scale calculations performed, i.e., up to 22% as reported by [22]. The high

deviations from the atomic scale data at higher thermal conductivity values correspond to low temperatures (data at 500 K [23], lower limit of applicability of the correlation) or to high Am contents between 15 and 25 at.% [23], outside the range of validity of the correlation.

5 CONCLUSION AND FUTURE DEVELOPMENTS

We presented in this deliverable the development and validation of original correlations for the thermal conductivity and melting temperature of minor actinide-bearing MOX $(U,Pu,Am,Np)O_{2-x}$. These are derived extending the correlations obtained in the project for U-Pu MOX fuels with the inclusion of the effect of Am and Np content, while preserving the physically-grounded formulation depending on the most relevant parameters. All the data available in the open literature, both experimental and from simulations (atomic scale modelling and CALPHAD calculations), were collected and selected sub-sets of experimental data were exploited as fitting datasets. This allowed us to extend the ranges of applicability of the correlations obtained up to significant Am and Np contents (10 at.% and 12 at.%, respectively) and to sufficiently high burnup (150 GWd/t_{HM}). However, the minor actinide content effect on the thermal properties of mixed oxides proves to be limited, at least in the aforementioned ranges (where data are currently available). The results yielded by the novel MA-MOX correlations are within the experimental uncertainties and the average deviations from the datasets considered are in line with or lower than the error of the existing correlations in the literature. This proves the validity of our approach and of the resulting correlations, which represent a step forward with respect to the state of the art.

To improve the correlations further, additional data are needed, especially to understand the impact of the deviation from stoichiometry and (high) plutonium content and to assess the impact of higher minor actinide contents. In addition, further investigations would be useful on high-porosity MOX (> 10% TD, of concern especially for the un-restructured zone of FBR and Gen IV fuels), in order to reduce the large deviations observed in the state-of-the-art data in this porosity range. Moreover, the evolution of thermal conductivity and melting temperature of both MOX and MA-MOX fuels at high burnup requires dedicated analyses, given the scarcity of experimental data and the current limitations of atomic scale simulations in this respect.

For future developments, results of atomic scale calculation and data from thermodynamic modelling could be exploited as part of the fitting dataset to refine the modelling of thermal properties and to further extend the ranges of validity of the correlations proposed. This type of calculations is very usefule to cover the compositions and conditions for which experimental information is currently missing or scarce (e.g., high temperatures > 2000 K, Pu contents > 40 at.%, heterogeneous MA content > 5 at.%).

Finally, the impact of minor actinide concentrations in oxide nuclear fuels could be assessed via grain-scale simulations based on rate theory approaches (exploiting e.g., the MFPR-F [54] and SCIANTIX [55] codes). These tools enable the evaluation of the density of lattice defects induced by self-irradiation, which deteriorates the thermal, and transport properties. This would allow us to refine the modelling of the burnup effect in both correlations. The analysis of the impact of fission products (and their compounds) on the microstructure and properties of mixed oxide nuclear fuels is of high interest to improve the models currently used in FPCs.

REFERENCES

[1] GIF (Generation IV International Forum), GIF R&D Outlook for Generation IV Nuclear Energy Systems - 2018 Update, 2018.

[2] GIF (Generation IV International Forum), Annual Report 2019, 2019.

[3] A. Magni, L. Luzzi, D. Pizzocri, A. Schubert, P. Van Uffelen, A. Del Nevo, Modelling of thermal conductivity and melting behaviour of minor actinide-MOX fuels and assessment against experimental and molecular dynamics data, J. Nucl. Mater. 557 (2021) 153312.

[4] J.-F. Babelot, N. Chauvin, Joint CEA/JRC Synthesis Report of the Experiment SUPERFACT 1, JRC-ITU-TN-99/03, 1999.

[5] K. Konno, T. Hirosawa, Melting temperature of irradiated fast reactor mixed oxide fuels, J. Nucl. Sci. Technol. 35 (1998) 494–501.

[6] M. Kato, K. Morimoto, H. Sugata, K. Konashi, M. Kashimura, T. Abe, Solidus and liquidus temperatures in the UO_2-PuO_2 system, J. Nucl. Mater. 373 (2008) 237–245.

[7] D. Prieur, R.C. Belin, D. Manara, D. Staicu, J.C. Richaud, J.F. Vigier, A.C. Scheinost, J. Somers, P. Martin, Linear thermal expansion, thermal diffusivity and melting temperature of Am-MOX and Np-MOX, J. Alloys Compd. 637 (2015) 326–331.

[8] K. Konno, T. Hirosawa, Melting temperature of mixed oxide fuels for fast reactors, J. Nucl. Sci. Technol. 39 (2002) 771–777.

[9] K. Tanaka, M. Osaka, S. Miwa, T. Hirosawa, K. Kurosaki, H. Muta, M. Uno, S. Yamanaka, Preparation and characterization of the simulated burnup americium-containing uranium-plutonium mixed oxide fuel, J. Nucl. Mater. 420 (2012) 207–212.

[10] M. Kato, K. Maeda, T. Ozawa, M. Kashimura, Y. Kihara, Physical properties and irradiation behavior analysis of Np- and Am-Bearing MOX Fuels, J. Nucl. Sci. Technol. 48 (2011) 646–653.

[11] K. Morimoto, M. Kato, H. Uno, A. Hanari, T. Tamura, H. Sugata, T. Sunaoshi, S. Kono, Preparation and characterization of (Pu, U, Np, Am, simulated FP)O_{2-x}, J. Phys. Chem. Solids. 66 (2005) 634–638.

[12] M. Kato, K. Morimoto, H. Sugata, K. Konashi, M. Kashimura, T. Abe, Solidus and liquidus of plutonium and uranium mixed oxide, J. Alloys Compd. 452 (2008) 48–53.

[13] R. Böhler, M.J. Welland, D. Prieur, P. Cakir, T. Vitova, T. Pruessmann, I. Pidchenko, C. Hennig, C. Guéneau, R.J.M. Konings, D. Manara, Recent advances in the study of the UO_2-PuO_2 phase diagram at high temperatures, J. Nucl. Mater. 448 (2014) 330–339.

[14] M. Strach, D. Manara, R.C. Belin, J. Rogez, Melting behavior of mixed U-Pu oxides under oxidizing conditions, Nucl. Instruments Methods Phys. Res. Sect. B Beam Interact. with Mater. Atoms. 374 (2016) 125–128.

[15] C.O.T. Galvin, P.A. Burr, M.W.D. Cooper, P.C.M. Fossati, R.W. Grimes, Using molecular dynamics to predict the solidus and liquidus of mixed oxides (Th,U)O_2, (Th,Pu)O_2 and (Pu,U)O_2, J. Nucl. Mater. 534 (2020) 152127.

[16] C. Guéneau, P. Fouquet-Métivier, P. Martin, R. Vauchy, M. Freyss, M.S. Talla Noutack, I. Cheik Njifon, Thermodynamic modelling of the (U-Pu-Am-O) system, INSPYRE Deliverable D1.1, 2019.

[17] A. Magni, T. Barani, A. Del Nevo, D. Pizzocri, D. Staicu, P. Van Uffelen, L. Luzzi, Modelling and assessment of thermal conductivity and melting behaviour of MOX fuel for fast reactor applications, J. Nucl. Mater. 541 (2020) 152410.

[18] P. Fouquet-Métivier, L. Medyk, R. Vauchy, P.M. Martin, L. Vlahovic, D. Robba, C. Guéneau, Melting behaviour of (U,Pu)O_2 SFRs fuels: influence of Pu and Am contents and oxygen stoichiometry, in: NuMat 2020 The Nuclear Material Conference, 26-30 October 2020, Online, 2020.

[19] K. Morimoto, M. Kato, M. Ogasawara, M. Kashimura, T. Abe, Thermal conductivities of (U,Pu,Am)O_2 solid solutions, J. Alloys Compd. 452 (2008) 54–60.

[20] K. Morimoto, M. Kato, M. Ogasawara, M. Kashimura, Thermal conductivities of hypostoichiometric (U,Pu,Am)O_{2-x} oxide, J. Nucl. Mater. 374 (2008) 378–385.

[21] K. Morimoto, M. Kato, M. Ogasawara, M. Kashimura, Thermal conductivity of (U,Pu,Np)O_2 solid solutions, J. Nucl. Mater. 389 (2009) 179–185.

[22] K. Kurosaki, J. Adachi, M. Katayama, M. Osaka, K. Tanaka, M. Uno, S. Yamanaka, Molecular dynamics studies of americium-containing mixed oxide fuels, J. Nucl. Sci. Technol. 43 (2006) 1224–1227.

[23] W. Li, J. Ma, J. Du, G. Jiang, Molecular dynamics study of thermal conductivities of ($U_{0.7-x}Pu_{0.3}Am_x$)O_2, J. Nucl. Mater. 480 (2016) 47–51.

[24] J.-M. Bonnerot, Propriétés thermiques des oxydes mixtes d'uranium et de plutonium, PhD Thesis, 1988.

[25] A. Magni, L. Luzzi, P. Van Uffelen, D. Staicu, P. Console Camprini, P. Del Prete, A. Del Nevo, Report on the improved models of melting temperature and thermal conductivity for MOX fuels and JOG, INSPYRE Deliverable D6.2, version 2, 2020.

[26] K. Yokohama, M. Watanabe, M. Kato, D. Tokoro, M. Sugimoto, Thermal conductivity measurement of high Am bearing mixed oxide fuel, in: NuMat 2020 The Nuclear Material Conference, 26-30 October 2020, Online, 2020.

[27] K. Morimoto, M. Kato, A. Komeno, M. Kashimura, Evaluation of thermal conductivity of (U,Pu, Am)O_{2-x}, Trans. Am. Nucl. Soc. 97 (2007) 618–619.

[28] European Commission, TRANSURANUS Handbook, Joint Research Centre, Karlsruhe, Germany, 2021.

[29] J. Fink, Thermophysical properties of uranium dioxide, J. Nucl. Mater. 279 (2000) 1–18.

[30] J.J. Carbajo, G.L. Yoder, S.G. Popov, V.K. Ivanov, A review of the thermophysical properties of MOX and UO_2 fuels, J. Nucl. Mater. 299 (2001) 181.

[31] L.J. Siefken, E.W. Coryel, E.A. Harvego, J.K. Hohorst, SCDAP/RELAP5/MOD 3.3 Code Manual, MATPRO - A Library of Materials Properties for Light-Water-Reactor Accident Analysis, 2001.

[32] K. Maeda, S. Sasaki, M. Kato, Y. Kihara, Behavior of Si impurity in Np-Am-MOX fuel irradiated in the experimental fast reactor Joyo, J. Nucl. Mater. 385 (2009) 178–183.

[33] K. Maeda, S. Sasaki, M. Kato, Y. Kihara, Short-term irradiation behavior of minor actinide doped uranium plutonium mixed oxide fuels irradiated in an experimental fast reactor, J. Nucl. Mater. 385 (2009) 413–418.

[34] K. Maeda, S. Sasaki, M. Kato, Y. Kihara, Radial redistribution of actinides in irradiated FR-MOX fuels, J. Nucl. Mater. 389 (2009) 78–84.

[35] K. Maeda, K. Katsuyama, Y. Ikusawa, S. Maeda, Short-term irradiation behavior of low-density americium-doped uranium-plutonium mixed oxide fuels irradiated in a fast reactor, J. Nucl. Mater. 416 (2011) 158–165.

[36] D. Manara, C. Ronchi, M. Sheindlin, M. Lewis, M. Brykin, Melting of stoichiometric and hyperstoichiometric uranium dioxide, J. Nucl. Mater. 342 (2005) 148–163.

[37] P. Martin, N. Chauvin, J.P. Ottaviani, D. Staicu, R. Calabrese, N. Vèr, G. Trillon, J. Klousal, A. Fedorov, M.A. Mignanelli, S. Portier, M. Verwerft, Preparing ESNII for HORIZON 2020 - Deliverable D7.5.1 - Catalog on MOX properties for fast reactors, ESNII+ Deliverable D7.5.1, 2017.

[38] MathWorks, MATLAB code, https://uk.mathworks.com/products/matlab (2019).

[39] The R Foundation, R version 3.5.1, https://www.r-project.org/ (2018).

[40] D. Staicu, E. Dahms, D. Manara, J.-Y. Colle, O. Benes, M. Marchetti, D. Robba, N. Chauvin, P. Martin, Preparing ESNII for HORIZON 2020 - Deliverable D7.4.1 - Measurement of properties of fresh Phenix fuel, ESNII+ Deliverable D7.4.1, 2017.

[41] F. De Bruycker, K. Boboridis, R.J.M. Konings, M. Rini, R. Eloirdi, C. Guéneau, N. Dupin, D. Manara, On the melting behaviour of uranium/plutonium mixed dioxides with high-Pu content: A laser heating study, J. Nucl. Mater. 419 (2011) 186–193.

[42] T. Hirosawa, I. Sato, Burnup dependence of melting temperature of FBR mixed oxide fuels irradiated to high burnup, J. Nucl. Mater. 418 (2011) 207–214.

[43] C.T. Walker, Assessment of the radial extent and completion of recrystallisation in high burnup UO_2 nuclear fuel by EPMA, J. Nucl. Mater. 275 (1999) 56–62.

[44] J. Noirot, L. Desgranges, J. Lamontagne, Detailed characterization of high burnup structures in oxide fuels, J. Nucl. Mater. 372 (2008) 318–339.

[45] F. Lemoine, D. Baron, P. Blanpain, Key parameters for the High Burnup Structure formation thresholds, in: LWR Fuel Perform. Meeting - Top Fuel, 26-29 September 2010, Orlando, Florida, USA, 2010.

[46] Y. Ida, Interionic repulsive force and compressibility of ions, Phys. Earth Planet. Inter. 13 (1976) 97–104.

[47] S.. Lemehov, V. Sobolev, P. Van Uffelen, Modelling thermal conductivity and self-irradiation effects in mixed oxide fuels, J. Nucl. Mater. 320 (2003) 66–76.

[48] M.W.D. Cooper, S.C. Middleburgh, R.W. Grimes, Modelling the thermal conductivity of $(U_xTh_{1-x})O_2$ and $(U_xPu_{1-x})O_2$, J. Nucl. Mater. 466 (2015) 29–35.

[49] K. Yamamoto, T. Hirosawa, K. Yoshikawa, K. Morozumi, S. Nomura, Melting temperature and thermal conductivity of irradiated mixed oxide fuel, J. Nucl. Mater. 204 (1993) 85–92.

[50] D. Staicu, E. Dahms, T. Wiss, O. Benes, J. Colle, Preparing ESNII for HORIZON 2020 - Deliverable D7.4.2 - Properties measurements on irradiated fuels (NESTOR 3), ESNII+ Deliverable D7.4.2, 2017.

[51] D. Staicu, E. Dahms, D. Manara, M. Marchetti, D. Robba, T. Wiss, B. Cremer, O. Dieste-Bianco, N. Chauvin, P. Martin, Preparing ESNII for HORIZON 2020 - Deliverable D7.3.4 - Characterization and measurement of properties of fresh TRABANT fuel, ESNII+ Deliverable D7.3.4, 2017.

[52] D. Staicu, M. Barker, Thermal conductivity of heterogeneous LWR MOX fuels, J. Nucl. Mater. 442 (2013) 46–52.

[53] P. Pernot, F. Cailliez, A critical review of statistical calibration/prediction models handling data inconsistency and model inadequacy, AIChE J. 63 (2017) 4642–4665.

[54] T.R. Pavlov, F. Kremer, R. Dubourg, A. Schubert, P. Van Uffelen, Towards a More Detailed Mesoscale Fission Product Analysis in Fuel Performance Codes: a Coupling of the TRANSURANUS and MFPR-F Codes, in: TopFuel2018 - React. Fuel Performance, 30 September - 04 October 2018, Prague, Czech Republic, 2018.

[55] D. Pizzocri, T. Barani, L. Luzzi, SCIANTIX: A new open source multi-scale code for fission gas behaviour modelling designed for nuclear fuel performance codes, J. Nucl. Mater. 532 (2020) 152042.